

Hydrothermal synthesis, structure and thermal stability of diamine templated layered uranyl-vanadates

M. Rivenet¹, N. Vigier, P. Roussel, F. Abraham

Unité de Catalyse et de Chimie du Solide, Equipe Chimie du Solide, UCCS UMR CNRS 8181, USTL, ENSC-B.P. 90108, 59652 Villeneuve d'Ascq Cedex, France.

Murielle.rivenet@ensc-lille.fr

Running Title :

Diamine templated layered uranyl-vanadates.

Figure for table contents

Keywords:

*Diamine uranyl vanadates, Crystal structure,
Hydrothermal synthesis, layered structure*

¹ To whom correspondence should be addressed; E-mail: Murielle.rivenet@ensc-lille.fr

Hydrothermal synthesis, structure and thermal stability of diamine templated layered uranyl-vanadates

M. Rivenet, N. Vigier, P. Roussel, F. Abraham

Unité de Catalyse et de Chimie du Solide, Equipe Chimie du Solide, UCCS UMR CNRS 8181, USTL, ENSCL-B.P. 90108, 59652 Villeneuve d'Ascq Cedex, France.

Abstract

Introduction

The solid state chemistry of uranyl – containing inorganic compounds is very rich in diversity. In particular, the association of hexavalent uranium polyhedra and oxoanion such as silicate, phosphate, vanadate, molybdate, tungstate. . . constitutes a true building set leading to structures with varied architectures and dimensionalities, although there is a tendency to form layered structure due to the presence of uranyl bonds that preclude the connection in a third dimension. The basic building units are the uranium polyhedron, which can be hexagonal bipyramid, pentagonal bipyramid or distorted octahedron and the oxoanion which can be tetrahedron, square bipyramid or octahedron. The structural arrangement depends on many factors, such as the U/oxoanion ratio, that influence the degree of polymerization between the uranium polyhedra which can be connected directly through equatorial oxygen atoms or through the oxo – anions polyhedra.

Our group of research mainly focuses on the solid state chemistry of uranyl-vanadates compounds [1-7]. In almost the studied oxides, the association of uranyl polyhedra through vanadate oxoanions leads to bi-dimensional anionic sheets with counteraction in the interlayer space. However in a recent paper, we described a novel three-dimensional open – framework uranyl-vanadate obtained using small monovalent ions (Li and Na) [8].

Owing to the potential applications for this type of materials (radioactive waste management, uranium geochemistry, ion-exchange and catalysis), a series of reactions was conducted in order to obtain new open-framework uranyl-vanadates. One approach for designing novel layered and microporous uranium-bearing materials is to exert influence over structural features through the introduction of templating agents. Amines have historically been used as charge balancing, space filling and templating agents in various systems including molybdate [9-13], phosphate [14-18], phosphite [19], selenate [20], selenite [21],

arsenate [17] sulfate [22-31] and fluoride containing compounds [18, 31-39] but organically templated uranyl-vanadates systems remained unexplored so far.

The materials described in the present paper were obtained by means of reactions of inorganic species and U/V ratio equal 1 with excess of amines under hydrothermal conditions. Two linear diamines of different length (1,2-ethylenediamine (*en*), 1,3-diaminopropane (*dap*)) and three cyclical diamines based upon piperazine (piperazine (*pip*), 1-methylpiperazine (*mpip*) and 1,4-diazabicyclo[2,2,2]octane (*dabco*)) were employed so as to vary the structures of the organic templates from a reaction to an other. Syntheses led to six new layered uranyl-vanadates which crystal structure and thermal behavior are reported herein.

Experimental

Synthesis

Uranyl nitrate ($\text{UO}_2(\text{NO}_3)_2 \cdot 6\text{H}_2\text{O}$ – Prolabo, R.P. normapur), vanadium oxide (V_2O_5 -Merck, Extra pur), concentrated chlorhydric acid (Carlo Erba, 37%, $d=1.186$) and amines (listed in Table 1) were used as received. For each synthesis the solutions were heated to 180°C in Teflon – lined 23mL digestion bombs for a time varying from 1 to 30 days. The resulting powders were collected after cooling to ambient temperature, filtration and washing with deionized water. Reaction yields were not quantitatively determined.

$(\text{NH}_4)_2[(\text{UO}_2)_2\text{V}_2\text{O}_8]$ (**1**) was synthesised using $\text{UO}_2(\text{NO}_3)_2 \cdot 6\text{H}_2\text{O}$ (301.3mg, 0.600mmol), V_2O_5 (54.6mg, 0.300mmol), 1,2 – ethylenediamine ($\text{C}_2\text{H}_8\text{N}_2$ - 90.2mg, 1.5mmol) and deionized water (15.1g, 840mmol). The mixture was heated at 180°C for 30 days. Absence of ammonium in the starting reactants indicates that the formation of ammonium ions must involve the *in situ* decomposition of ethylenediamine. Amines decomposition under hydrothermal conditions has previously been observed using pyridine [40], imidazole [41], and guanidinium amines [42-45]. It is worth noting that we were able to obtain $(\text{NH}_4)_2[(\text{UO}_2)_2\text{V}_2\text{O}_8]$ using a more direct source of ammonium cations.

$(\text{H}_2\text{en})[(\text{UO}_2)_2\text{V}_2\text{O}_8]$ (**2**) was prepared by hydrothermal reaction using a mixture of $\text{UO}_2(\text{NO}_3)_2 \cdot 6\text{H}_2\text{O}$ (301.3mg, 0.600mmol), V_2O_5 (54.6mg, 0.300mmol), 1,2 – ethylenediamine ($\text{C}_2\text{H}_8\text{N}_2$ - 90.2mg, 1.5mmol) and deionized water (15.1g, 840mmol) added with chlorhydric acid (HCl - 109.4mg, 3mmol). Time of synthesis was limited to 1 day in order to avoid the ethylenediamine decomposition.

(H_{2dap})[(UO₂)₂V₂O₈] (**3**), (H_{2pip})[(UO₂)₂(VO₄)₂]·0.8H₂O (**4**), (H_{2dmpip})[(UO₂)₂V₂O₈] (**5**) and (H_{2dabco})[(UO₂)₂(VO₄)₂] (**6**) were obtained by conducting hydrothermal reactions at 180°C for 2 days using a mixture of UO₂(NO₃)₂·6H₂O (301.3mg, 0.600mmol), V₂O₅ (54.6mg, 0.300mmol), HCl (109.4mg, 3mmol), deionized water (15.1g, 840mmol) and, respectively, C₃H₁₀N₂ (111.2mg, 1.5mmol), C₄H₁₀N₂ (129.2mg, 1.5mmol), C₅H₁₂N₂ (150.3mg, 1.5mmol) and C₆H₁₂N₂ (168.3mg, 1.5mmol). During the synthesis of **5** under the hydrothermal conditions used, some 1-methylpiperazine (*mpip*) dismutated in 1,-dimethylpiperazine (*dmpip*) and piperazine (*pip*). The single crystals grew from *mdpip* when the presence of *pip* in the remaining solution was unambiguously proved by ¹³C RMN.

The purity of the compounds was checked using X-ray powder diffraction. The X-ray powder patterns of the bulk samples can be fully indexed on the basis of the theoretical data calculated from the crystal structure results which evidences that pure phases are obtained. For compounds **1**, **4**, **5** and **6** crystals suitable for single crystal X-ray diffraction experiments have been isolated under optical microscope.

Crystal structure determination

Selected crystals of **1**, **4**, **5** and **6** were mounted on a glass fiber and aligned on a Bruker SMART CCD X-ray diffractometer. Intensities were collected at room temperature using MoK α ($\lambda = 0.71073 \text{ \AA}$) radiation selected by a graphite monochromator. The individual frames were measured using a ω -scan technique. Omega rotation and acquisition time were fixed at 0.3° and 20 s per frame, respectively. 1800 frames were collected in order to cover the full sphere. The Bruker program SAINT [46] was used for intensity data integration and correction for Lorentz, polarisation and background effects. After data processing, absorption corrections were performed using a semi-empirical method based on redundancy with the SADABS program [47]. Details of the data collection and refinement are given in Table 2.

The crystal structures were determined in the centrosymmetric space groups $P2_1/c$ for **1**, $P2_1/b$ for **5** and $C2/m$ for both **4** and **6**. A non-conventional setting was chosen for **5** so that the layers described hereafter are always in the (1 0 0) plane for **1**, **5**, **2** and **3** compounds. The heavy atoms (U, V) positions were established by direct methods using SIR97 program [48]. The oxygen, nitrogen and carbon atoms were localised from difference Fourier maps. The last cycles of refinement included atomic positions and anisotropic displacement

parameters ADP for all atoms, excepted for partially occupied sites. Full-matrix least-squares structure refinements against F were carried out using the JANA2000 program [49]. The atomic positional parameters and displacement parameters are given in Table 3 – compound **1**, Table 4 – compound **5** and Table 5 – compounds **4** and **6**. Some selected interatomic distances are reported in Table 6 – compounds **1** and **5**, and Table 7 – compounds **4** and **6**.

As no suitable crystals could be found for the **2** and **3** samples, crystal structure models were checked using X-ray powder diffraction data. The data were collected by means of a Huber G670 diffractometer using an asymmetric Guinier flat sample transmission geometry, equipped with a 2D detector (Image Plate) covering the 2θ range [6 – 100°]. The $(\text{H}_2en)[(\text{UO}_2)_2\text{V}_2\text{O}_8]$ and $(\text{H}_2dap)[(\text{UO}_2)_2\text{V}_2\text{O}_8]$ samples were exposed, respectively, for one hour and half an hour to a monochromatized Cu-K α_1 radiation obtained with a Germanium Johanson monochromator. For the ethylenediamine containing compound **2**, the powder was dehydrated before measurement by heating the sample at 200°C for 1 hour. For the two compounds, structural models containing only the uranium – vanadium – oxygen sheets with distances constrained to the values calculated for the compounds **5** and **1**, respectively are used and led to the results reported in Table 8.

For compound **2**, the **b** and **c** parameters correspond to a carnotite – type layer, however the space group symmetry operations are incompatible with such a structure and as we could not find any structurally related compound, we attempted to solve the structure of compound **2** by *ab initio* procedures. The pattern decomposition option of the JANA2000 package [49] was used to extract corrected structure factors from a limited region of the diffractogram ($6 < 2\theta < 60^\circ$). The pattern was fit without any structural model by refining the overall parameters: background, unit-cell parameters, zero-point error, peak shape (pseudo-Voigt). The refinement converged to $R_{wp} = \text{xx}$ and $R_p = \text{xx}\%$. A total of **xxx** reflections were used as input to the direct-methods SIR97 program [48]. The positions of two U atoms were derived from this method. At this stage, the positions of the V atoms were deduced from a difference-Fourier map. Then, after refining the heavy atoms position and ADP, another difference-Fourier map revealed O atoms. At this stage we used soft constraints in the U – O and V – O bonds to avoid the structure blow up and to keep a reasonable geometry for the anionic sheets. Unfortunately, probably due to the high contrast between the U and (C – N – H) atoms of the amines, we were not able to see these last types of atomic species in a last difference-Fourier map. Without these "light" atoms and refining all positional parameters R_{wp} dropped to 1.80 %. Refining isotropic temperature factors freely resulted in some

negative values. It is well known that temperature factors, for complex structures with heavy cations and medium resolution X-ray powder data, are quite unreliable. Hence, we decided to refine an overall isotropic temperature factor for U and V atoms and to fix an overall temperature factor for the oxygen atoms. The refined positional parameters are reported in Table 9.

For the compound **3**, the values of the cell parameters and the XRD pattern are very similar to those of uranyl vanadates of divalent A cations built from carnotite type layers. The space group deduced from the X – ray powder pattern indexation, *Pm*cn, is adopted for A = Ca [50], Mn, Co [51], Ni, Cd, Zn [52]. The precise lattice parameters were obtained from profile matching and, using the structural model of the divalent carnotite-type compounds layers, the reliability factors reported in Table 8 are obtained.

High temperature X – ray diffraction

The high temperature X-ray powder diffraction patterns were recorded using a Guinier Lenné moving film camera. The samples were deposited on the sample holder (gold grid) using an ethanol slurry which yielded, upon evaporation, a regular layer of powdered compound. The high temperature X-ray diffraction patterns were recorded in the temperature range from 20 to 600°C with a heating rate in the range [12 – 15° h⁻¹].

Thermal analysis

The thermal analyses were performed on a Setaram TG-DT 2-16.18 apparatus. Analyses were undertaken in air, in the temperature range from 20 to 600°C, with a heating rate of 300° h⁻¹, in platinum crucibles.

Results

Cation coordination polyhedra

For all the studied compounds, each of the uranium atom is strongly bonded to two oxygen atoms forming a nearly linear uranyl cation (UO₂)²⁺ with a O – U – O bond angle ranging from 178.6(4) to 179.5(3)° and U – O bond lengths ranging from 1.775(8) to 1.816(6) Å (average value of 1.79(2) Å). The uranyl cations are coordinated by five oxygen atoms located in the equatorial plane which forms [UO₇] pentagonal bipyramids. The equatorial oxygen ligands show significant variations with U – O distances ranging from 2.295(6) to 2.458(3) Å. However, the average value, 2.36(6) Å, is in good agreement with the average

bond length of 2.37(9) Å calculated for uranyl polyhedra of numerous well – refined structures [53].

The vanadium atoms of structures **1**, **2**, **3** and **5** are pentacoordinated by five oxygen atoms in a square pyramidal arrangement. Two VO₅ square pyramids related by an inversion centre share an O – O edge to form a V₂O₈ dimeric unit. Within the VO₅ square pyramids, the apical V – O bond is shorter than the vanadium – oxygen distances of the square base. This vanadyl V – O bond distance is close to that calculated in various carnotite-type compounds [54] and V₂O₅ [55].

In structures **4** and **6**, the vanadium atoms occupy one crystallographic site with tetrahedral environment. The tetrahedra are slightly distorted with V – O distances in the range from 1.721(7) to 1.763(5) Å when the oxygen atoms are shared with a UO₇ polyhedron and shorter distances with O(5) atom not involved in uranium coordination, 1.62(1) and 1.611(6) Å for **4** and **6**, respectively.

Bond – valence sums were calculated using parameters given by Burns *et al.* [53] for U – O bonds and by Brese and O’Keeffe [56] for V – O bonds. Calculations resulted in values ranging from 6.00(2) to 6.19(3) *v.u.* for U⁶⁺ and from 5.08(5) to 5.14(4) *v.u.* for V⁵⁺ with oxygen valences ranging from 1.57(2) to 2.18(2) *v.u.*. The lowest sums correspond to O atoms not shared between UO₇ and VO₄ or VO₅ polyhedra.

Structural connectivity

The structural building unit block, with labelled scheme, constituted from two edge-shared UO₇ pentagonal bipyramids and two edge-shared VO₅ square pyramids is shown on Fig. 1 for compounds **1**, **2** and **5**.

Compound **1** is isotypic with the mineral carnotite K₂[(UO₂)₂V₂O₈] and other A₂[(UO₂)₂V₂O₈]·nH₂O compounds where A is a monovalent ion [45], CsUNbO₆ [57] and A₂[(UO₂)₂Cr₂O₈]·nH₂O (A=K, Rb Cs) [58]. The structural arrangement between the edge-shared dimers, V₂O₈, and the edge- and corner- shared pentagonal bipyramids, UO₇, further linked by edge-sharing, forms sheets of composition [(UO₂)₂V₂O₈]²⁻ parallel to (1 0 0) (Fig. 2b). The ammonium anions are located in the interlayer space and insure the cohesion of the structure.

Compound **3** is built from the same layers. The layers packing along *a*-axis depends upon the interleaving cation. In **1**, as in almost the monovalent containing

$A_2[(\text{UO}_2)_2\text{V}_2\text{O}_8]\cdot x\text{H}_2\text{O}$ compounds, adjacent layers noted P are deduced by a translation, resulting in the simple PPPP sequence (Fig. 3a). In compound **3** there is a second layer, labelled b, deduced from P by a (1 0 0) mirror plane. P and b layers alternate to yield a PbPb sequence (Fig. 3b). Such a sequence was previously evidenced in $A[(\text{UO}_2)_2\text{V}_2\text{O}_8]\cdot x\text{H}_2\text{O}$ compounds containing a divalent A cation [50-52].

Using the description developed by Burns *et al.* [59], the francevillite anion topology of the $[(\text{UO}_2)_2\text{V}_2\text{O}_8]^{2-}$ sheets is represented in Fig. 2a. Compounds **2** and **5** are built from sheets with the same anion topology and with the same occupation of pentagons by U, squares by V and empty triangles, but, in contrast with all the carnotite-type layer containing compounds described up today (Fig. 2b), half of the V_2O_8 units are reversed compared to the P sheets (Fig. 2c). A V_2O_8 dimer can be referenced as *ud* with a tetragonal pyramid that point *up* and one *down*. In P layers the dimers alternate, along [0 1 0], to form the isomer *ud/du*, in opposite, the new anionic layer, labelled P' hereafter, represents the *ud/ud* geometrical isomer. In compound **5**, a layer b' is deduced from P' by a two fold axis running along c axis so as the stacking sequence is P'b'P'b' (Fig. 3d) while the stacking sequence in structure **2** can be described as P'P'P'P' (Fig. 3c). Along [0 0 1] the V_2O_8 dimmers are parallel.

Compounds **4** and **6** are isotypic and contain the same $[(\text{UO}_2)_2(\text{VO}_4)_2]^{2-}$ layer built from $(\text{UO}_5)_\infty$ zig-zag chains of edge shared UO_7 pentagonal bipyramids running down the *b*-axis further connected by VO_4 tetrahedra. The uranyl vanadate layer has the uranophane sheets anion topology (Fig. 4) adopted by many mineral or synthetic inorganic or hybrid organic-inorganic uranyl compounds. In **4** and **6**, all the tetrahedra that share edges with one side of a uranyl chain point down (*d*), and all the tetrahedra along the other side point up (*u*) which corresponds to the geometrical isomer *du/du* as defined by Locock *et al.* [60]. The three dimensional structure results from the alternate stacking of inorganic layers and sheets of protonated amines and occluded water molecules.

It should be noticed that with triethylamine, Locock and Burns [17] obtained the same structural arrangement but with another geometrical isomer of the uranyl arseniate layer whereas with *dabco* molecules an autunite-type uranyl arseniate layer is formed.

Interlayer space occupation

In order to study the role of amine on the structural arrangement of the uranyl – vanadates, the location and connectivity of amines in the interlayer space was systematically investigated for the single crystal studied compounds.

Projected along [1 0 0], the interleaving NH_4^+ cations in **1** appears at the centre of the inoccupied triangles of the francevillite anion – type topology (Fig. 5). The NH_4^+ ions occupy the same position than the alkali atoms in the $A_2[(\text{UO}_2)_2\text{V}_2\text{O}_8]$ compounds. Investigation of the N – O distances evidenced eight N – O contacts in a continuous range from 2.8 to 3.3 Å without any O – N – O angle corresponding to a tetrahedral coordination involving hydrogen bonds, so the pseudo – alkali character of the ammonium cation dominates in this compound. Fig. 6 shows the variation of the inter-layer distance $a\sin\beta$ for the $A_2[(\text{UO}_2)_2\text{V}_2\text{O}_8]$ compounds with the ionic radii of the 8 – coordinated A^+ ions [61]. Using the value of ionic radius reported by Khan and Bauer [62] for the 8-coordinated NH_4^+ (1.66 Å), the corresponding point does not fit with this straightforward variation, so according to Shannon [61] for the 6-coordination, we should conclude that NH_4^+ is not different in size from Rb^+ .

Although in **2** and **3** the diprotonated amines could not be localised one can imagine that they separate the inorganic layers from one another creating spacing of approximately 6.98 and 7.37 Å between uranium atom planes and stabilize the structures, both through balancing the negative charge of the inorganic layer, and donating hydrogen bonds.

In **5**, the $[\text{H}_2\text{dmpip}]^{2+}$ cations, with a chair conformation, are aligned along [0 0 1] in the space between the $[(\text{UO}_2)_2\text{V}_2\text{O}_8]^{2-}$ layers. The mean plane of the diamines is inclined of about 45° from the layer. As evidenced on Fig. 5, the arrangement of the diamines in the interlayer space is incompatible with the *ud/du* isomer. The two nitrogen atoms of the $[\text{H}_2\text{dmpip}]^{2+}$ cation donate their hydrogen bonds to the apical oxygen atoms O(2) of two parallel uranyl-vanadate layers with a N1 – – – O2 distance of 2.98(2) Å.

In **4** and **6**, the $[\text{H}_2\text{pip}]^{2+}$ and $[\text{H}_2\text{dabco}]^{2+}$ cations reside between the inorganic layers and are located above the VO_4 tetrahedra of the $[(\text{UO}_2)_2(\text{VO}_4)_2]^{2-}$ uranophane layers that points down. In **4**, the interleaving $[\text{H}_2\text{pip}]^{2+}$ molecules lie almost parallel to (1 0 0) plane with no strong hydrogen bonds with the uranyl vanadate layer : instead, the shortest N – – – O distances, 2.71(2) Å involves an oxygen of the interleaving water molecules. The $[\text{H}_2\text{pip}]^{2+}$ molecules adopt a boat conformation which can be present in two possible orientations related by a mirror parallel to (0 0 1). Thus, the site occupancy factors for the C(1), C(2) and N(1) atoms, located in a general position, were fixed at 0.5. In **6**, the pseudo-trigonal $[\text{H}_2\text{dabco}]^{2+}$ cations (Fig. 7) can be found with two possible orientations modelled by half occupying the

general positions of C(1), C(2) and N(1) atoms. Moreover, a disorder presented by the C(3) – C(4) group, was taken in account by fixing at 0.25 the site occupancy for C(3) and C(4) atoms, located in a general position. The $[\text{H}_2\text{dabco}]^{2+}$ molecule are slightly distorted with C(1) – C(2) and C(3) – C(4) bond lengths respectively equivalent to 1.67(2) and 1.64(5) Å and N(1) – C bond lengths varying within the range [1.40 – 1.55] Å. The cations are oriented such as their ammonium moities are directed toward the corner sharing oxygen atoms O(3) of the $\text{VO}_4 - \text{UO}_7$ units with a strong N – – – O(3) hydrogen bond lying along the N – N axis of 2.78(1) Å. That indicates the presence of a three-dimensional hydrogen bonds network that constrains the $[\text{H}_2\text{dabco}]^{2+}$ cations to lie almost perpendicular to the layers as previously observed in diamine templated uranium sulfates [26].

Thermal behaviour

For compound **1**, a one-step decomposition from $(\text{NH}_4)_2[(\text{UO}_2)_2\text{V}_2\text{O}_8]$ to $(\text{UO}_2)_2\text{V}_2\text{O}_7$ [63] corresponding to 6.1% weight loss in accordance with the 6.5% theoretical loss is observed between 375 and 470°C on the TGA curve. The thermal behavior is confirmed by high temperature X-ray diffraction experiment.

For all the amine bearing materials (**2** to **6**), the decomposition of the amine and the modification of the uranyl – vanadate arrangement occur in several steps between 280 and 550°C. On the high temperature X-ray diffraction patterns a non – crystalline zone is observed between the starting uranyl – vanadate and the final product $(\text{UO}_2)_2\text{V}_2\text{O}_7$ [61]. The total weight losses are in agreement with the calculated values for the transformation from (*Diamine*)[uranyl-vanadate] to $(\text{UO}_2)_2\text{V}_2\text{O}_7$ (exp. / theor. (%): 9.0/9.4 – 11.3/10.9 – 11.5/12.0 – 14.8/14.9 – 14.0/14.6 for structures **2** – **6** respectively).

Conclusion.

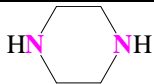
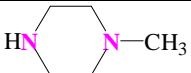
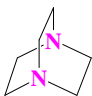
For the five studied structure directing diamines, uranyl vanadates layers with formula $(\text{UVO}_6)^{2-}$ are formed. Two types of layers were obtained. For compounds **1**, **2**, **3** and **5**, the $[(\text{UO}_2)_2\text{V}_2\text{O}_8]^{2-}$ layers are similar to that of the mineral carnotite with two geometrical isomers distinguished by the orientations of the V_2O_8 units. For compounds **4** and **6**, the uranophane-type layers are built from chains of edge-shared UO_7 pentagonal bipyramids connected through VO_4 tetrahedra. In all the compounds, the diprotonated amines reside between the inorganic layers, balancing charge and donating hydrogen bonds to the layers. For all

compounds, thermal decomposition led to the divanadate $(\text{UO}_2)_2\text{V}_2\text{O}_7$. Further experiments using other amine structure directing agents to built three-dimensional uranyl-vanadate frameworks are in progress.

Acknowledgment.

The authors gratefully thank Catherine Méliet (UCCS, USTL) and Marc Bria (SCM RMN-RPE, USTL) for their assistance in collecting and interpreting the ^{13}C NMR spectra. The "Fonds Européen de Développement Régional (FEDER)", "CNRS", "Région Nord Pas-de-Calais" and "Ministère de l'Education Nationale de l'Enseignement Supérieur et de la Recherche" are acknowledged for fundings of X-ray diffractometers.

Table 1 : Amine molecules of the studied $\text{UO}_3\text{-V}_2\text{O}_5$ -amine systems.

Name	Formula	Origin	Compound
1,2 – Ethylenediamine (<i>en</i>)	$\text{H}_2\text{N}(\text{CH}_2)_2\text{NH}_2$	ACROS, 99%, d=0.899	1 and 2
1,3 – Diaminopropane (<i>dap</i>)	$\text{H}_2\text{N}(\text{CH}_2)_3\text{NH}_2$	ACROS, 99%, d=0.870	3
Piperazine (<i>pip</i>)		ACROS, 99%	4
1 – Methylpiperazine (<i>mpip</i>)		ACROS, 99%	5
1,4 – Diazabicyclo[2,2,2]octane (<i>dabco</i>)		ACROS, 97%	6

Compound n°	1	4	5	6
Chemical formula	(NH ₄) ₂ [(UO ₂) ₂ V ₂ O ₈]	(H ₂ <i>pip</i>)[(UO ₂) ₂ (VO ₄) ₂].0,8H ₂ O	(H ₂ <i>dmpip</i>)[(UO ₂) ₂ V ₂ O ₈]	(H ₂ <i>dabco</i>)[(UO ₂) ₂ (VO ₄) ₂]
Crystallographic data				
Formula weight (g.mol ⁻¹)	806	872.5	886.1	884.1
Crystal system	monoclinic	monoclinic	monoclinic	monoclinic
Space group	<i>P2₁/c</i>	<i>C2/m</i>	<i>P2₁/b</i>	<i>C2/m</i>
Unit – cell dimensions (Å)	<i>a</i> = 6.894(2) <i>b</i> = 8.384(3) <i>c</i> = 10.473(4) <i>β</i> = 106.066(5)	<i>a</i> = 15.619(2) <i>b</i> = 7.1802(8) <i>c</i> = 6.9157(8) <i>β</i> = 101.500(2)	<i>a</i> = 9.315(2) <i>b</i> = 8.617(2) <i>c</i> = 10.5246(2) <i>γ</i> = 114.776(2)	<i>a</i> = 17.440(2) <i>b</i> = 7.1904(9) <i>c</i> = 6.8990(8) <i>β</i> = 98.196(2)
Cell volume (Å ³)	581.7(4)	760.0(2)	767.0(2)	856.3(2)
Z	2	2	2	2
Density, calculated (g.cm ⁻³)	4.600(3)	3.814(1)	3.838(1)	3.4279()
<i>F</i> (000)	696	768	784	780
Intensity collection				
Wavelength (Å)	0.71069 (MoK α)	0.71069 (MoK α)	0.71069 (MoK α)	0.71069 (MoK α)
θ range (deg)	3.07 – 28.67	3.01 – 23.27	2.41 – 27.95	2.98 – 28.44
Data collected	- 9 ≤ <i>h</i> ≤ 9 - 11 ≤ <i>k</i> ≤ 11 - 13 ≤ <i>l</i> ≤ 13	- 17 ≤ <i>h</i> ≤ 17 - 7 ≤ <i>k</i> ≤ 7 - 7 ≤ <i>l</i> ≤ 7	- 12 ≤ <i>h</i> ≤ 12 - 13 ≤ <i>k</i> ≤ 13 - 10 ≤ <i>l</i> ≤ 10	- 23 ≤ <i>h</i> ≤ 23 - 9 ≤ <i>k</i> ≤ 9 - 9 ≤ <i>l</i> ≤ 9
No. of reflections measured	4549	2005	5425	3549
No. of independent reflections	1364	590	1633	1105
Redundancy	3.335	3.40	3.32	3.212
No. of unique reflections (<i>I</i> > 3 σ (<i>I</i>))	1186	530	1250	1027
μ (MoK α) (mm ⁻¹)	29.373	22.502	22.296	19.971
<i>T</i> _{min} / <i>T</i> _{max}	0.466	0.367	0.680	0.202
<i>R</i> (<i>F</i> ²) _{int}	0.0397	0.0313	0.0492	0.0319
Refinement				
No. of parameters	83	62	110	77
Weighting scheme	1/ σ^2	1/ σ^2	1/ σ^2	1/ σ^2
<i>R</i> (<i>F</i>) obs/all	0.0276/0.0340	0.0214/0.0240	0.0332/0.0502	0.0238/0.0250
w <i>R</i> (<i>F</i>) obs/all	0.0296/0.0304	0.0244/0.0249	0.0291/0.0306	0.0300/0.0302
Max, min $\Delta\rho$ (e. Å ⁻³)	1.97/ - 1.84	0.78/ - 1.01	2.32/ - 1.57	1.89/ - 1.20

Table 2 : Crystal data, intensity collection and structure refinement parameters for (NH₄)₂[(UO₂)₂V₂O₈] (**1**), (H₂*pip*)[(UO₂)₂(VO₄)₂].0,8H₂O (**4**), (H₂*dmpip*)[(UO₂)₂V₂O₈] (**5**) and (H₂*dabco*)[(UO₂)₂(VO₄)₂] (**6**).

Table 3. Atomic coordinates and isotropic displacement parameters (in Å²) for (NH₄)₂[(UO₂)₂V₂O₈] (**1**).

Atom	Wyck.	x	y	z	U _{eq}
U1	4e	0.01539(4)	0.47727(3)	0.81974(2)	0.0110(2)
V1	4e	0.1147(2)	0.8516(2)	0.0557(2)	0.0122(4)
O1	4e	0.2776(8)	0.4265(7)	0.8795(5)	0.020(2)
O2	4e	-0.2457(9)	0.5260(6)	0.7598(5)	0.019(2)
O3	4e	0.0406(8)	0.0607(6)	0.1079(5)	0.016(2)
O4	4e	0.0418(8)	0.6553(6)	-0.0044(4)	0.016(2)
O5	4e	0.3484(9)	0.8708(7)	0.0648(5)	0.025(2)
O6	4e	0.0930(8)	0.7909(6)	0.2192(5)	0.016(2)
N1	4e	-0.458(2)	0.7697(9)	0.8626(7)	0.029(3)

Table 4. Atomic coordinates and isotropic displacement parameters (in Å²) for (H₂dmpip)[(UO₂)₂V₂O₈] (**5**)

Atom	Wyck.	x	y	z	U _{eq}
U1	4e	0.48421(4)	0.47738(4)	-0.31760(3)	0.0125(2)
V1	4e	0.4327(2)	0.1248(2)	-0.4674(2)	0.0149(7)
O1	4e	0.6969(8)	0.5718(8)	-0.3076(7)	0.024(3)
O2	4e	0.2702(7)	0.3856(8)	-0.3308(7)	0.020(3)
O3	4e	0.5371(8)	0.0699(8)	-0.5981(6)	0.017(3)
O4	4e	0.5028(8)	0.3475(8)	-0.5114(6)	0.016(3)
O5	4e	0.2473(7)	0.0417(8)	-0.4949(7)	0.022(3)
O6	4e	0.4657(8)	0.1971(7)	-0.2998(6)	0.019(3)
N1	4e	0.004(2)	0.488(2)	-0.3662(9)	0.061(6)
C1	4e	0.095(2)	0.648(2)	-0.424(2)	0.041(5)
C2	4e	-0.113(2)	0.350(2)	-0.436(2)	0.043(5)
C3	4e	-0.015(2)	0.487(2)	-0.222(2)	0.062(8)

Table 5. Atomic coordinates and isotropic displacement parameters (in Å²) for (H₂*pip*)[(UO₂)₂(VO₄)₂].0,8H₂O (**4**) (bold type) and (H₂*dabco*)[(UO₂)₂(VO₄)₂] (**6**) (italic type).

Atom	Site	Occ.	x	y	z	U _{eq/ iso} *
U1	4i		0.75640(3)	0	-0.11646(6)	0.0118(2)
<i>U1</i>	<i>4i</i>		<i>0.75602(2)</i>	<i>0</i>	<i>-0.11813(3)</i>	<i>0.0138(2)</i>
V1	4i		0.7204(2)	0	-0.6690(2)	0.0108(6)
<i>V1</i>	<i>4i</i>		<i>0.71988(7)</i>	<i>0</i>	<i>-0.6700(2)</i>	<i>0.0138(3)</i>
O1	4i		0.8722(5)	0	-0.036(1)	0.020(3)
<i>O1</i>	<i>4i</i>		<i>0.8588(3)</i>	<i>0</i>	<i>-0.0535(8)</i>	<i>0.027(2)</i>
O2	4i		0.6409(5)	0	-0.191(2)	0.026(3)
<i>O2</i>	<i>4i</i>		<i>0.6528(3)</i>	<i>0</i>	<i>-0.1811(8)</i>	<i>0.027(2)</i>
O3	4i		0.7838(5)	0	-0.435(1)	0.020(3)
<i>O3</i>	<i>4i</i>		<i>0.7763(3)</i>	<i>0</i>	<i>-0.4412(7)</i>	<i>0.020(2)</i>
O4	8j		0.7433(4)	-0.1807(7)	-0.8236(7)	0.021(2)
<i>O4</i>	<i>8j</i>		<i>0.7428(2)</i>	<i>-0.1799(5)</i>	<i>-0.8221(5)</i>	<i>0.024(2)</i>
O5	4i		0.6179(6)	0	-0.659(2)	0.032(3)
<i>O5</i>	<i>4i</i>		<i>0.6289(4)</i>	<i>0</i>	<i>-0.6494(9)</i>	<i>0.038(2)</i>
O6w	4g	0.42(2)	0.5	-0.184(2)	0	0.014(6)*
N1	8j	0.5	0.504(2)	-0.386(2)	-0.667(2)	0.025(4)*
C1	8j	0.5	0.532(2)	-0.432(2)	-0.673(2)	0.022(5)*
C2	8j	0.5	0.482(2)	-0.304(2)	-0.543(2)	0.026(5)*
<i>N1</i>	<i>8j</i>	<i>0.5</i>	<i>0.0660(5)</i>	<i>-0.037(2)</i>	<i>0.453(2)</i>	<i>0.033(3)*</i>
<i>C1</i>	<i>8j</i>	<i>0.5</i>	<i>0.9325(9)</i>	<i>0.153(3)</i>	<i>0.371(2)</i>	<i>0.059(7)</i>
<i>C2</i>	<i>8j</i>	<i>0.5</i>	<i>0.0182(8)</i>	<i>0.118(2)</i>	<i>0.296(3)</i>	<i>0.068(7)</i>
<i>C3</i>	<i>8j</i>	<i>0.25</i>	<i>0.040(2)</i>	<i>0.163(4)</i>	<i>0.447(6)</i>	<i>0.054(9)*</i>
<i>C4</i>	<i>8j</i>	<i>0.25</i>	<i>0.946(2)</i>	<i>0.154(5)</i>	<i>0.451(7)</i>	<i>0.047(9)*</i>

Table 6. Principal interatomic distances (Å) for **1** and **5**.

Compound 1		Compound 5	
U1 – O1	1.793(5)	U1 – O1	1.802(7)
U1 – O2	1.782(6)	U1 – O2	1.816(6)
U1 – O3 ^{iv}	2.295(6)	U1 – O3 ⁱ	2.340(6)
U1 – O4 ⁱ	2.338(5)	U1 – O4	2.368(7)
U1 – O4 ⁱⁱ	2.356(5)	U1 – O4 ⁱⁱⁱ	2.319(7)
U1 – O6 ⁱ	2.369(5)	U1 – O6	2.356(7)
U1 – O6 ⁱⁱⁱ	2.342(5)	U1 – O6 ⁱⁱ	2.327(7)
V1 – O3 ^v	1.946(5)	V1 – O3	1.857(8)
V1 – O3 ^v	1.899(5)	V1 – O3 ^{iv}	1.940(8)
V1 – O4	1.784(5)	V1 – O4	1.809(7)
V1 – O5	1.596(6)	V1 – O5	1.594(6)
V1 – O6	1.832(6)	V1 – O6	1.853(6)
		V1 – V1 ^{iv}	2.988(3)
		N1 – O2	2.98(2)
		N1 – C1	1.42(2)
		N1 – C2	1.43(2)
		N1 – C3	1.53(2)
		C1 – C2 ^{vi}	1.48(2)

Symmetry codes for **1** (i) $-x, -y, 1-z$; (ii) $-x, 1-y, 1-z$; (iii) $x, 3/2-y, 1/2+z$; (iv) $x, 1/2-y, 1/2+z$ (v); $-x, 1-y, -z$; (vi) $-1+x, 1/2-y, 3/2+z$; (vii) $-1-x, -y, 1-z$; for **5** (i) $1-x, 1/2-y, 1/2+z$; (ii) $x, 1/2+y, -1/2-z$; (iii) $1-x, 1-y, -1-z$; (iv) $1-x, -y, -1-z$; (v) $1-x, 1/2-y, -1/2+z$; (vi) $-x, 1-y, -1-z$

Table 7. Principal interatomic distances (Å) for **4** and **6**.

Compound 4		Compound 6	
U1 – O1	1.775(8)	U1 – O1	1.784(5)
U1 – O2	1.783(8)	U1 – O2	1.791(5)
U1 – O3	2.326(7)	U1 – O3	2.306(5)
U1 – O4 ⁱ	2.448(5)	U1 – O4 ⁱ	2.456(4)
U1 – O4 ⁱⁱ	2.330(5)	U1 – O4 ⁱⁱ	2.339(4)
U1 – O4 ⁱⁱⁱ	2.330(5)	U1 – O4 ⁱⁱⁱ	2.339(4)
U1 – O4 ^{iv}	2.448(5)	U1 – O4 ^{iv}	2.456(4)
V1 – O3	1.721(7)	V1 – O3	1.737(5)
V1 – O4	1.763(5)	V1 – O4	1.747(4)
V1 – O4 ^v	1.763(5)	V1 – O4 ^v	1.747(4)
V1 – O5	1.62(1)	V1 – O5	1.613(7)
C1 – C2	1.59(2)	C1 – C2 ^{vii}	1.67(2)
		C3 – C4 ^{xiv}	1.64(5)
N1 ^{xiv} – C1	1.38(2)	N1 ^{xii} – C1	1.47(2)
N1 ^{xii} – C2	1.54(2)	N1 ^v – C2	1.40(2)
		N1 – C3	1.51(3)
		N1 – C4 ^x	1.55(4)
N1 ⁱ – O6w	2.71(2)	N1 ^{vii} – O3	2.78(1)
N1 ^{xii} – O6w	2.71(2)	N1 ^{viii} – O3	2.78(1)

Symmetry codes (i) $-x, -y, 1-z$; (ii) $3/2-x, -1/2-y, -1-z$; (iii) $3/2+x, 1/2-y, -1+z$; (iv) $1/2+x, 1/2-y, 1+z$; (v) $1/2+x, 1/2-y, z$; (vi) $3/2-x, -1/2-y, -2-z$; (vii) $1-x, -y, -z$; (viii) $1+x, -y, z$; (ix) $2+x, -y, 1+z$; (x) $1+x, -y, 1+z$; (xi) $3/2+x, 1/2-y, z$; (xii) $1-x, -y, 1-z$; (xiii) $x, -y, 1+z$; (xiv) $-1-x, -y, -z$; (xv) $-1/2+x, 1/2-y, z$; (xvi) $2-x, -y, 1-z$

Table 8 : Structure refinement parameters for (H_{2en})[(UO₂)₂V₂O₈] (**2**) and (H_{2dap})[(UO₂)₂V₂O₈] (**3**)

Compound n ^o	2	3
Chemical formula	(H _{2en})[(UO ₂) ₂ V ₂ O ₈]	(H _{2dap})[(UO ₂) ₂ V ₂ O ₈]
Crystallographic data		
Formula weight (g.mol ⁻¹)	832	846.1
Crystal system	monoclinic	orthorhombic
Space group	<i>P</i> 21/a	<i>P</i> mcn
Unit – cell dimensions (Å)	<i>a</i> = 13.9816(6) <i>b</i> = 8.6165(3) <i>c</i> = 10.4237(3) γ = 93.125(3)	<i>a</i> = 14.7363(8) <i>b</i> = 8.6379(4) <i>c</i> = 10.4385(4)
Cell volume (Å ³)	1253.91(9)	1327.5(2)
Z	4	4
Density, calculated (g.cm ⁻³)	4.406	4.232
Refinement		
R _p / R _w p	0.0133/0.0180	0.0168/0.0258
R _{obs} / R _w obs	0.0634/0.0573	0.0811/0.0815
R _{all} / R _w all	0.0679/0.0579	0.0959/0.0850
R _{exp}	0.0341	0.0382

Table 9. Atomic coordinates and isotropic displacement parameters (in Å²) for (H₂en)[(UO₂)₂V₂O₈] (**2**).

Atom	Wyck.	x	y	z	U _{iso/eq}
U1	4e	0.2367(4)	-0.2646(9)	0.2617(3)	0.009(2)
U2	4e	0.2576(5)	-0.236(1)	0.6282(3)	0.009(2)
V1	4e	0.276(2)	0.107(2)	0.470(2)	0.009(2)
V2	4e	0.679(2)	0.386(3)	0.092(2)	0.009(2)
O1	4e	0.3849(6)	-0.232(3)	0.608(3)	0.006
O2	4e	0.1306(4)	-0.242(1)	0.650(2)	0.006
O3	4e	0.3649(3)	-0.259(3)	0.257(4)	0.006
O4	4e	0.1086(4)	-0.2723(9)	0.265(2)	0.006
O5	4e	0.241(2)	-0.0941(9)	0.4378(3)	0.006
O6	4e	0.387(2)	0.144(6)	0.441(5)	0.006
O7	4e	0.738(2)	0.5924(9)	0.0464(3)	0.006
O8	4e	0.570(2)	0.402(5)	0.053(5)	0.006
O9	4e	0.2202(8)	0.198(7)	0.3497(9)	0.006
O10	4e	0.7336(3)	0.463(1)	0.248(2)	0.006
O11	4e	0.267(2)	0.321(5)	0.5411(9)	0.006
O12	4e	0.2627(5)	0.036(2)	0.638(2)	0.006

References

- 1 I. Duribreux, C. Dion, M. Saadi, F. Abraham, *J. Solid State Chem.* **146** (1999) 258.
- 2 C. Dion, S. Obbade, E. Raekelboom, M. Saadi, F. Abraham, *J. Solid State Chem.* **155** (2000) 342.
- 3 M. Saadi, C. Dion, F. Abraham, *J. Solid State Chem.* **150** (2000) 72.
- 4 S. Obbade, C. Dion, L. Duvieubourg, M. Saadi, F. Abraham, *J. Solid State Chem.* **173** (2003) 1.
- 5 I. Duribreux, M. Saadi, S. Obbade, C. Dion, F. Abraham, *J. Solid State Chem.* **172** (2003) 351.
- 6 S. Obbade, C. Dion, M. Saadi, F. Abraham, *J. Solid State Chem.* **177** (2004) 1567.
- 7 S. Obbade, C. Dion, M. Saadi, S. Yagoubi, F. Abraham. *J. Solid State Chem.* **177** (2004) 3909.
- 8 S. Obbade, C. Dion, M. Rivenet, M. Saadi, F. Abraham. *J. Solid State Chem.* **177** (2004) 2058.
- 9 P.S. Halasyamani, R.J. Francis, S.M. Walker, D. O'Hare, *Inorg. Chem.* **38** (1999) 271.
- 10 S.V. Krivovichev, P.C. Burns, *J. Solid State Chem.* **170** (2003) 106.
- 11 S.V. Krivovichev, C.L. Cahill, E.V. Nazarchuk, P.C. Burns, T. Armbruster, W. Depmeier, *Microporous and Mesoporous Materials* **78** (2005) 209.
- 12 S.V. Krivovichev, P.C. Burns, T. Armbruster, E.V. Nazarchuk, W. Depmeier, *Microporous and Mesoporous Materials* **78** (2005) 217.
- 13 S.V. Krivovichev, T. Armbruster, D.Y. Chernyshov, P.C. Burns, E.V. Nazarchuk, W. Depmeier, *Microporous and Mesoporous Materials* **78** (2005) 225.
- 14 R.J. Francis, J. Drewitt, P.S. Halasyamani, C. Ranganathachar, D. O'Hare, W. Clegg, S.J. Teat, *Chem. Commun.* (1998) 279.
- 15 J.A. Danis, W.H. Runde, B. Scott, J. Fettinger, B. Eichhorn, *Chem. Commun.* (2001) 2378.
- 16 J.A. Danis, H.T. Hawkins, B.L. Scott, W.H. Runde, B.E. Scheetz, B.W. Eichhorn, *Polyhedron* **19** (2000) 1551.
- 17 A.J. Locock, P.C. Burns, *J. Solid State Chem.* **177** (2004) 2675.
- 18 M.B. Doran, C.L. Stuart, A.J. Norquist, D. O'Hare, *Chem. Mater.* **16** (2004) 565.
- 19 M. Doran, S.M. Walker, D. O'Hare, *Chem. Commun.* (2001) 1988.

- 20 S.V. Krivovichev, V. Kahlenberg, I.G. Tananaev, R. Kaindl, E. Mersdorf, B.F. Myasoedov, *J. Am. Chem. Soc.* **127** (2005) 1072.
- 21 P.M. Almond, T.E. Albrecht – Schmitt, *Inorg. Chem.* **42** (2003) 5693.
- 22 M.B. Doran, A.J. Norquist, D. O'Hare, *Inorg. Chem.* **42** (2003) 6989.
- 23 A.J. Norquist, M.B. Doran, P.M. Thomas, D. O'Hare, *Dalton Trans.* (2003) 1168.
- 24 A.J. Norquist, M.B. Doran, P.M. Thomas, D. O'Hare, *Inorg. Chem.* **42** (2003) 5949.
- 25 A.J. Norquist, M.B. Doran, D. O'Hare, *Solid State Sciences* **5** (2003) 1149.
- 26 A.J. Norquist, P.M. Thomas, M.B. Doran, D. O'Hare, *Chem. Mater.* **14** (2002) 5179.
- 27 M. Doran, A.J. Norquist, D. O'Hare, *Chem. Comm.* (2002) 2946.
- 28 P.M. Thomas, A.J. Norquist, M.B. Doran, D. O'Hare, *J. Mater. Chem.* **13** (2003) 88.
- 29 M.B. Doran, A.J. Norquist, C.L. Stuart, D. O'Hare, *Acta Crystallogr.* **E60** (2004) m996; M.B. Doran, A.J. Norquist, D. O'Hare, *Acta Crystallogr.* **E59** (2003) m762; M.B. Doran, A.J. Norquist, D. O'Hare, *Acta Crystallogr.* **E59** (2003) m765; M.B. Doran, A.J. Norquist, D. O'Hare, *Acta Crystallogr.* **E59** (2003) m373; C.L. Stuart, M.B. Doran, A.J. Norquist, D. O'Hare, *Acta Crystallogr.* **E59** (2003) m446.
- 30 A.J. Norquist, M.B. Doran, D. O'Hare, *Inorg. Chem.* **44** (2005) 3837.
- 31 M.B. Doran, B.E. Cockbain, A.J. Norquist, D. O'Hare, *Dalton Trans.* (2004) 3810.
- 32 X. Wang, J. Huang, A.J. Jacobson, *J. Am. Chem. Soc.* **124** (2002) 15190.
- 33 R.J. Francis, P.S. Halasyamani, J.S. Bee, D. O'Hare, *J. Am. Chem. Soc.* **121** (1999) 1609.
- 34 R.J. Francis, P.S. Halasyamani, D. O'Hare, *Angew. Chem. Int. Ed.* **37** (1998) 2214.
- 35 S. Allen, S. Barlow, P.S. Halasyamani, J.F.W. Mosselmans, D. O'Hare, S.M. Walker, R.I. Walton, *Inorg. Chem.* **39** (2000) 3791.
- 36 R.J. Francis, P.S. Halasyamani, D. O'Hare, *Chem. Mater.* **10** (1998) 3131.
- 37 S.M. Walker, P.S. Halasyamani, S. Allen, D. O'Hare, *J. Am. Chem. Soc.* **121** (1999) 10513.
- 38 C.L. Cahill, P.C. Burns, *Inorg. Chem.* **40** (2001) 1347.
- 39 P.S. Halasyamani, S.M. Walker, D. O'Hare, *J. Am. Chem. Soc.* **121** (1999) 7415.
- 40 A.M. Chippindale, R.L. Walton, *J. Chem. Soc. Chem. Commun.* (1994) 2453.
- 41 A.M. Chippindale, A.R. Cowley, R.L. Walton, *J. Mater. Chem.* **6** (1996) 611.
- 42 J.C. Trombe, P. Thomas, C. Brouca – Cabarrecq, *Solid State Sciences* **3** (2001) 309.
- 43 Z. Bircsak, W.T.A. Harrison, *Acta Crystallogr.* **C54** (1998) 1383.
- 44 F. Fourcade – Cavillou, J.C. Trombe, *Solid State Sciences* **4** (2002) 1199
- 45 M. Saadi, Thesis, Lille, 1994.

- 46 SAINT Plus Version 6.22, Bruker Analytical X – ray Systems, Madison, WI, 2001.
- 47 SADABS Version 2.03: Bruker Analytical X – ray Systems, Madison, WI, 2001.
- 48 A. Altomare, G. Cascaro, G. Giacovazzo, A. Guargliardi, M.C. Burla, G. Polidori, M. Gamalli, *J. Appl. Crystallogr.* **27** (1994) 135
- 49 V. Petricek, M. Dusek, JANA2000, Institute of Physics, Praha, Czech Republic, 2005.
- 50 C. Frondel, D. Riska, J. W. Frondel, *U. S. Geol. Surv. Bull.* **1036 – G** (1956) 91.
- 51 M. Saadi, Thesis, El Jadida, Morocco, 2001.
- 52 F. Cesbron, *Bull. Soc. Fr. Minéral. Cristallogr.* **93** (1973) 320.
- 53 P.C. Burns, R.C. Ewing, F.C. Hawthorne, *Can. Miner.* **35** (1997) 1551.
- 54 F. Abraham, C. Dion, M. Saadi, *J. Mater Chem.* **3(5)** (1993) 459.
- 55 R. Enjalbert, J. Galy, *Acta Crystallogr.* **C42** (1986) 1467.
- 56 N. E. Brese, M. O'Keeffe, *Acta Crystallogr.* **B47** (1991) 192.
- 57 M. Gasperin, *Acta Crystallogr.* **C43** (1987) 404.
- 58 A. J. Locock, S. Skanthakumar, P. C. Burns, L. Soderholm, *Chem. Mater.* **16** (2004) 1384.
- 59 P.C. Burns, M.L. Miller and R.C. Ewing, *Can. Mineral.* **34** (1996) 845, P.C. Burns, *Can. Mineral.* **43** (2005) 1839.
- 60 A.J. Locock and P.C. Burns, *J. Solid State Chem.* 176 (2003) 18.
- 61 R. D. Shannon, *Acta Crystallogr.* **A32** (1976) 751.
- 62 A. A. Khan, W. Baur, *Acta Crystallogr.* **B28** (1972) 683.
- 63 N. Tancret, S. Obbade, F. Abraham, *Eur. J. Solid State.Inog. Chem.* **32** (1995) 195; A.M. Chippindale, P. J. Dickens, G. J. Flynn, G. P. Stuttard, *J. Mater. Chem.* **5** (1995) 141.

Figure caption.

Fig. 1: The structure building unit block formed of two edge-shared UO_7 pentagonal bipyramids and two edge-shared VO_5 square pyramids further connected by edge with the labelled scheme for a) compounds **1** and **5**, b) compound **2**.

Fig. 2: The francevillite anion topology (**a**) and the uranyl vanadate layers in carnotite – type compounds: (**b**) *ud/du* isomer layers P in $\text{M}^+ -$, $\text{M}^{2+} -$ or 1, 3 – diaminopropane – containing compounds; (**c**) *ud/ud* isomer layers P' in ethylenediamine – and 1,4 – dimethylpiperazine – containing compounds.

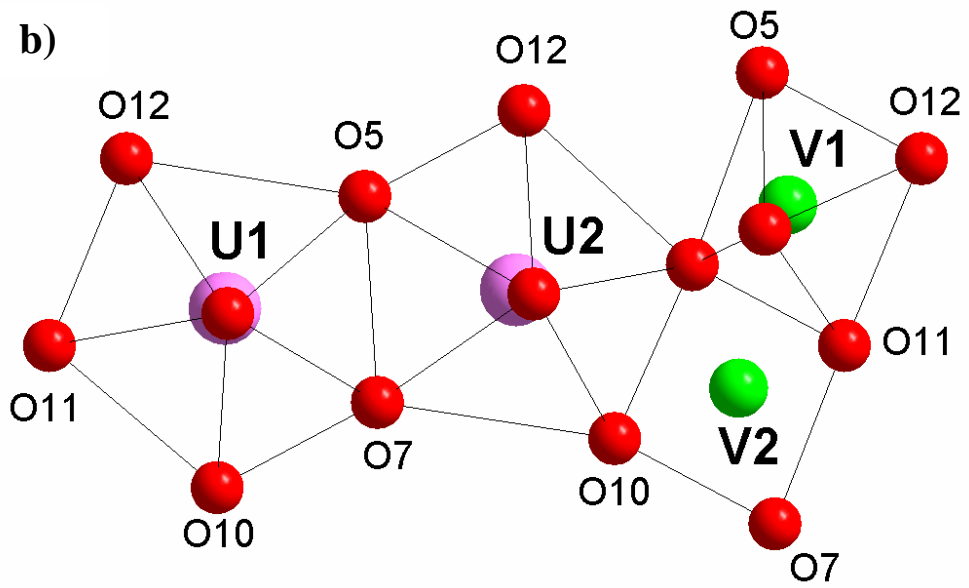
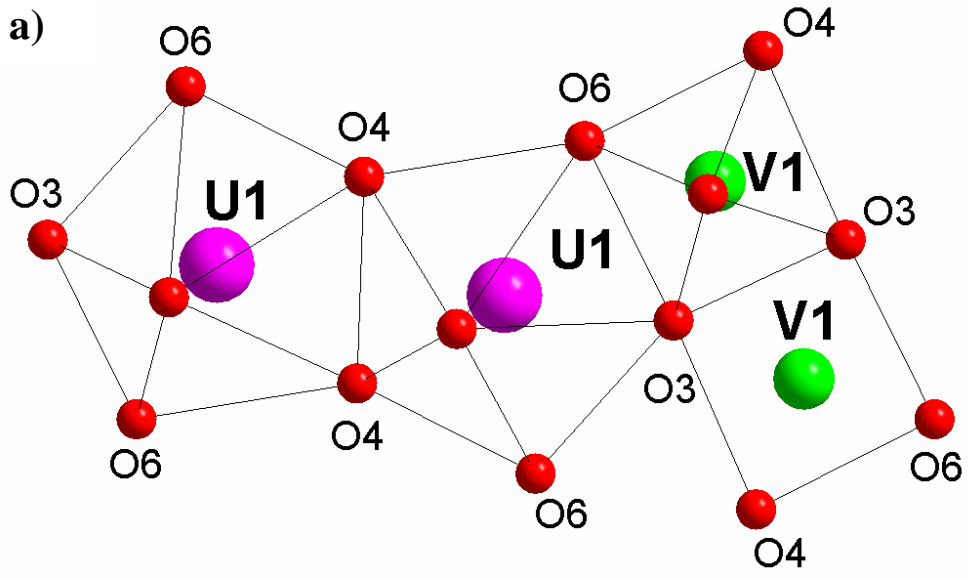
Fig. 3: Stacking of the P and P' layers in carnotite type compounds containing monovalent ions and **1** (**a**), divalent inorganic ions and **3** (**b**), 1,4 – dimethylpiperazine **5** (**c**) and ethylenediamine (not localized from X – ray powder diffraction data) **6** (**d**).

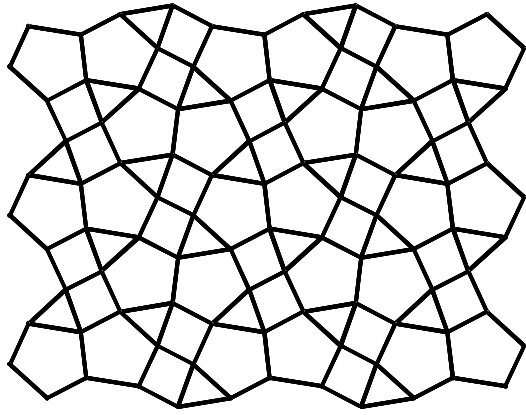
Fig. 4: The uranophane type uranyl vanadate sheet in the structure of 4 and 6.

Fig. 5: Localisation of the ammonium cation above the *ud/du* geometrical isomer layer in **1** (**a**), dimethylpiperazine ions above the *ud/ud* geometrical isomer layer in **5** (**b**), piperazine and *dabco* above the uranophane-type layer in **4** and **6**, (**c**) and (**d**), respectively.

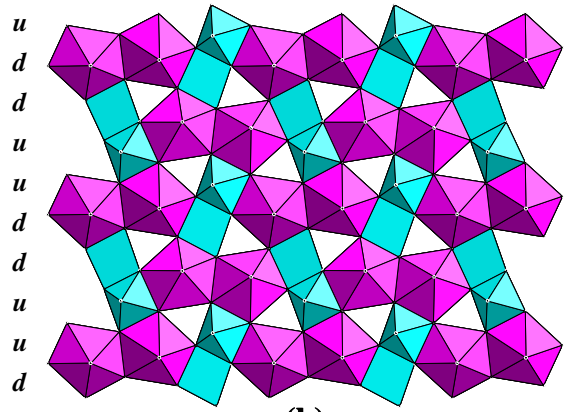
Fig. 6: Variation of the interlayer distance versus the ionic radii of 8-coordinated monovalent ion $\text{A}_2[(\text{UO}_2)_2\text{V}_2\text{O}_8]$ compounds built on carnotite-type layers.

Fig. 7: One orientation of the pseudo-trigonal $[\text{H}_2\text{dabco}]^{2+}$ cations showing the disorder presented by the C(3) – C(4) group. The general positions of C(1), C(2) and N(1) atoms are half occupied.

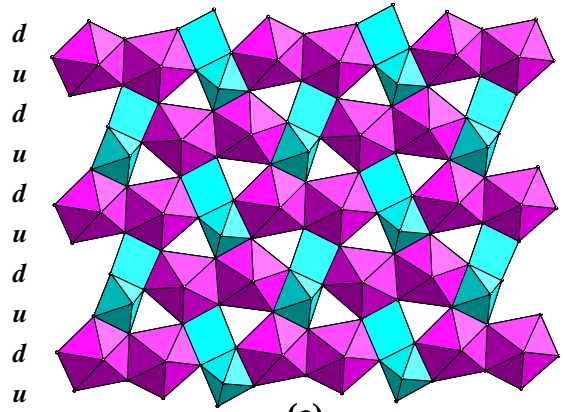




(a)



(b)



(c)

